Liquid-State Properties of a One-Component Plasma

Jérôme Daligault*

Theoretical Division, Los Alamos National Laboratory, Los Alamos, New Mexico 87545, USA

(Received 10 November 2005; published 17 February 2006)

As a consequence of strong collective behavior, the microscopic dynamics of the one-component plasma (OCP) differs significantly from that of ordinary liquids. We show that, when particle caging dominates, the OCP transport coefficients nevertheless satisfy universal laws satisfied by dense ordinary fluids: the Stokes-Einstein relation, the Arrhenius law of viscosity, and several excess-entropy scaling relations. These results extend to long-range interaction potentials, the unifying description of atomic transport in condensed matter.

DOI: 10.1103/PhysRevLett.96.065003 PACS numbers: 52.27.Gr, 52.25.Fi

An important model in the study of strongly coupled Coulomb systems is the classical one-component plasma (OCP), which consists of a single species of charged particles (charge q, mass m) immersed in a uniform, neutralizing background [1]. The OCP plays a conceptual role similar to that filled by the hard-sphere model in the theory of simple liquids, and can also be seen as a limiting case of real matter under extreme conditions (e.g., atomic nuclei in white dwarfs interiors). The thermodynamic state of the OCP is characterized by the coupling parameter $\Gamma = q^2/ak_BT$, where $a = (4\pi n/3)^{-1/3}$ is the Wigner-Seitz radius, n is the particle density, and T is the temperature. As Γ increases, the OCP shows transitions from a nearly collisionless, gaseous regime for $\Gamma \ll 1$ continuously through an increasingly correlated, liquidlike regime to the Wigner crystallization into a lattice near $\Gamma_m = q^2/ak_BT_m = 175$.

The goal of this study is to clarify how this transition to a liquid-state regime occurs. We show that, despite the differences in the microscopic dynamics of the OCP and ordinary liquids, the OCP behaves much like a liquid in the $\Gamma_l \leq \Gamma \leq \Gamma_m$ range, with $\Gamma_l \simeq 50$. We show that, in this range, the OCP transport properties obey well-established laws satisfied by ordinary liquids, such as the Arrhenius law for the viscosity, the Stokes-Einstein relation between self-diffusion and shear viscosity, and several ''universal'' excess-entropy scaling relations. To this end, we have performed molecular dynamics (MD) simulations to determine, to unprecedented accuracy and Γ-range, the OCP pair-distribution function $g(r)$, the velocity autocorrelation function (VAF), the self-diffusion coefficient D, and shear-viscosity coefficient η by evaluating the appropriate Green-Kubo expressions. The present results are important from both practical and fundamental point of views. They can indeed be used to construct models of transport in more complex strongly coupled Coulomb systems (e.g., dense multicomponent plasmas), and support the continued search for a unifying description of atomic transport in condensed matter.

As a consequence of the infinite range of the Coulomb potential, each particle of the OCP interacts not just with a limited number of neighbors, as is the case for a particle in an ordinary fluid, but with all the other particles. Any charge fluctuation can give rise to propagating, high-frequency, collective modes of frequency $\omega_p = (4\pi nq^2/m)^{1/2}$ in the infinite wavelength limit. The fluid OCP therefore exhibits dynamical behavior not encountered in ordinary monatomic fluids as illustrated in Fig. 1. The figure shows results of MD simulations for the VAF of the OCP and of two common kinds of monatomic liquids at different thermodynamic states, Lennard-Jones liquids [2] and liquid alkali metals [3]. At low enough coupling, all VAFs decay monotonically, a behavior implying the absence of many-body correlation effects. At higher coupling (large density and/or low temperature), another common behavior is the appearance of a negative correlation region. This is the manifestation of the ''cage effect'': owing to pronounced structural correlations, each particle finds itself trapped for some period of time in the cage formed by its immediate neighbors, rebounding against it and thereby slowing down the diffusive motion. For the OCP, negative correlations appear at $\Gamma = \Gamma_l \sim 50$. The cage effect in the OCP was recently studied and quantified with MD [4]; the authors estimated the time $T_d = 0.13\exp(\Gamma^{0.35})/\omega_p$ needed for a cage to be decorrelated, i.e., for 90% probability that half of the particles' original neighbors leave their surroundings. In liquids, a characteristic frequency for the oscillatory motion of a caged particle in the potential well produced by the other particles is the Einstein frequency Ω_E. For the OCP, $\Omega_E = \omega_p/\sqrt{3} < \omega_p$, and one therefore expects caging to be strongly affected by the coupling of the single-particle motion to collective density fluctuations [4]. This is indeed the case as revealed by the marked oscillatory nature at a frequency $\simeq 0.9\omega_p$ of the OCP VAF for $\Gamma \geq 10$; such sustained oscillations are not seen in ordinary fluids. Notice also that the lowest minimum of $Z(t)$ is attained by its first minimum in ordinary liquids but by its second minimum in the OCP. For strongly coupled liquids, the VAF frequency spectra reveal a broad low-frequency peak, which is attributed to coupling to acoustic shear modes [5,6]. For the OCP this peak arises

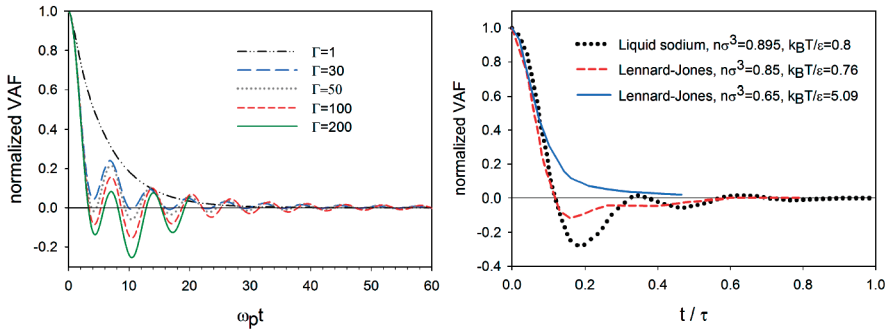

FIG. 1 (color). Normalized VAF at different thermodynamic states of the OCP (left panel), Lennard-Jones liquids (from [2]), and metal liquids [3]. ϵ, σ, and $\tau = (m\sigma^2/\epsilon)^{1/2}$ are, respectively, the depth and first zero of the pair potentials and the time unit.

when $\Gamma \geq 100$ in addition to the marked high-frequency peak at $\simeq 0.9\omega_p$.

Our MD simulations are based on the particle-particle-particle-mesh algorithm with periodic boundary conditions and were performed in the canonical ensemble using a Nosé-Hoover thermostat. The time step is $\delta t = 0.01/\omega_p$, which ensures good energy conservation ($\Delta E/E \sim 10^{-6}$). The present results were obtained with $N = 1024$ particles using the following procedure. After a long equilibration of 10^5 time steps, a run of length $t = 30 \times 1310.72\omega_p^{-1}$ was performed; each run was then divided into 30 statistically independent ensembles of length $t = 1310.72\omega_p^{-1}$, i.e., much larger than typical correlation times. Our simulations cover the $0.2 \leq \Gamma \leq 250$ range; when $\Gamma > \Gamma_m$ the system is in a supercooled liquid state. Interesting aspects of MD simulations that we had to face at high Γ are worth mentioning here. Despite careful equilibration phases and long simulation times, we found that results for the diffusion coefficient depend upon the initial particle configuration when $\Gamma > 150$. The system remains in the initial metastable state with respect to the equilibrium thermodynamic state over times much longer than the simulation time. As a consequence, averages over phase space are not the same as time averages; the ergodicity is broken. For instance, with a crystal lattice (bcc or fcc) in the fluid phase $\Gamma < \Gamma_m$, the system fails to melt over the simulation time (it is a superheated solid) unless $\Gamma < 150$ when the lattice is very unstable and melts during the equilibration phase. Correspondingly, as expected for a perfect lattice, the self-diffusion obtained is nearly zero. Similarly, when starting with a random particle configuration at $\Gamma > \Gamma_m$, the system stays in a metastable supercooled liquid state over the time scale of the simulation, unless $\Gamma(>250)$ is large enough for crystal nucleation to occur, resulting in the drop of the diffusion coefficient. (We are presently investigating the OCP nucleation dynamics and reserve the results for future publication.) The results in Fig. 2 for $\Gamma > \Gamma_m$ are representative of the supercooled liquid OCP.

Figure 2 shows the MD results for the reduced self-diffusion $D^* = D/a^2\omega_p$ and viscosity $\eta^* = \eta/mna^2\omega_p$. Both D^* and ν^* were fitted to a rational function $f(\Gamma) = \sum_{i=1}^{3} a_i\Gamma^i / \sum_{i=1}^{3} b_i\Gamma^i$ with the parameters a_i and b_i given in Table I. Results for η^* do not agree well with previous calculations (see [7] for a review), which we believe to be due to the combination of finite-size effects and poor statistics. The latter indeed use fewer particles, fewer statistically independent ensembles, and fewer time steps. The viscosity curve presents a behavior typical of ordinary fluids. In a fluid, transport of momentum occurs not only by the bodily movement of particles, but also by the action of interparticle forces at a distance. At small coupling, the former mechanism is predominant and, as in a gas, the OCP viscosity increases with temperature. At intermediate coupling, $10 \leq \Gamma \leq 50$, the two mechanisms contribute with similar magnitude, resulting in a shallow minimum near $\Gamma \simeq 25$. When $\Gamma \geq 50$ the viscosity decreases with increasing temperature (or lowering density), in an Arrhenius-type relation $\eta^* = Ae^{B\Gamma}$, with $A \simeq 0.10$ and $B \simeq 0.008$. This behavior, which occurs when caging dominates, can be understood within Eyring's theory of atomic transport in liquids [8]. In this approach, based on the absolute reaction rates theory, a cage is represented by an energy barrier ΔG. The frequency at which a caged particle can overcome and pass the potential barrier is

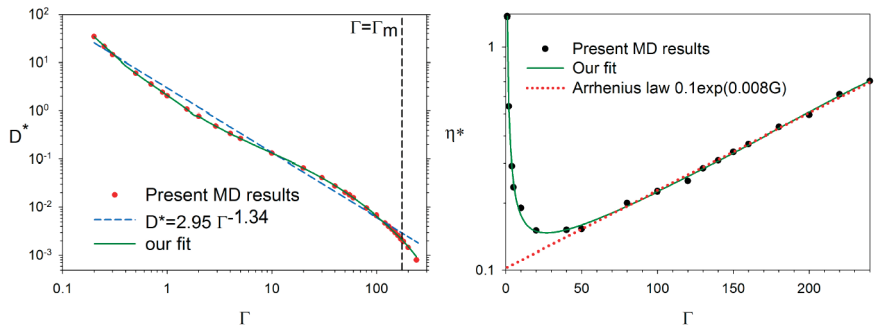

FIG. 2 (color). OCP reduced self-diffusion D^* (log-log) and shear-viscosity η^* (log-linear) and fitting formulas (solid line). The dashed line is the fitting formula of Hansen *et al.* [18]. The dotted line is the Arrhenius relation $\eta^* = 0.10\exp(0.008\Gamma)$.

TABLE I. Fitting parameters. For D^* the Γ range is split into two parts, (a) $\Gamma \leq 2$ and (b) $\Gamma \geq 2$.

	a_0	a_1	a_2	a_3	b_0	b_1	b_2	b_3
D^* (a)	−0.73	3.90	0.49	−0.27	0.042	−0.502	1.34	0.74
D^* (b)	59.74	3.11	0.001 37	-2.4×10^{-5}	−32.1	56.25	1.24	0.037
η^*	1.60	0.24	6×10^4	-1.8×10^{-6}	−1.216	2.58	−0.014	2.255×10^{-5}

given by the rate equation $\nu = \kappa k_B T \exp(-\Delta G/k_B T)/h$, where h is the Planck constant and κ is the probability that the particle jumps to the neighboring cavity when it reaches the activated state. The Eyring model leads to the Arrhenius behavior $\eta \simeq \delta n k_B T/\nu = \delta h n \times \exp(\Delta G/k_B T)/\kappa$, where δ is a geometrical factor. Comparison with our fit allows one to estimate the activation energy; one obtains $\Delta G \simeq 1.4 k_B T_m$, in good agreement with activation energies measured in liquid metals [9]. Using our MD results for $g(r) \equiv \exp[-w(r)/k_B T]$, one can estimate the cage radius, i.e., the average distance d^* separating the center of a cage to the position of the activated state by solving $\Delta G = w(d^*)$, which yields $d^*(\Gamma) = 1.4a \pm 2\%$. Since δ is not known *a priori*, one cannot infer an absolute value for the frequency ν of jumps between cages. The ratio $\nu(\Gamma)/\nu(\Gamma_m)$, however, is accessible, and allows one to compare the time scale of the dynamics of caging in a liquid at Γ with the liquid OCP at Γ_m; for instance, $\nu(50) \simeq 10\nu(\Gamma_m)$, i.e., at $\Gamma = 50$ jumps between cavities occur 10 times more often than at $\Gamma = \Gamma_m$. Moreover, this ratio is directly comparable with the ratio $T_d(\Gamma_m)/T_d(\Gamma)$ [4] of the time needed for a cage to be decorrelated (see above). We find a striking agreement (within 5%) between the two ratios. This is a strong evidence of the relevance of Eyring's model, and thereby that caging is the mechanism of transport at $\Gamma \geq \Gamma_l$.

It is well known that the Stokes-Einstein relation provides an intimate connection between the self-diffusion and shear-viscosity coefficients of dense fluids,

$$D\eta \frac{R}{k_B T} \simeq \frac{2}{q\pi}, \tag{1}$$

where R is an effective molecular radius and q a numerical constant. This relation was first derived from a purely hydrodynamic description, using Stokes's law for the viscous drag on a moving sphere of radius R in a fluid with shear viscosity η. The resulting constant q depends on the choice of boundary conditions at the surface of the sphere, $q = 6$ with sticking boundary conditions and $q = 4$ with slipping boundary conditions. Surprisingly enough, Eq. (1) is found to work fairly well even for one-component dense fluids, where any distinction between the diffusing particle and those of the surrounding fluid disappears. Several microscopic theoretical models were able to give a sounder justification of Eq. (1) in simple liquids [10,11]. In particular, Gaskell and Miller [11] derived a model for the VAF $Z(t) \simeq (\frac{1}{2\pi})^2 \int d\mathbf{q} f(q)[C_L(q,t) + 2C_T(q,t)]$ in terms of the Fourier transform $f(q)$ of a step-function "form factor" $f(r) = \theta(a - r)$, and of C_L and C_T, the longitudinal- and transverse-current correlation functions, respectively. This model provides a justification of the VAF frequency spectra of both dense ordinary liquids [5] and strongly coupled OCP [6]: C_T reproduces the broad low-frequency peak while, for the OCP, C_L reproduces the high-frequency peak. The model also results in a generalized Stokes-Einstein relation,

$$D = \frac{k_B T}{m} \int_0^\infty Z(t)dt \simeq \frac{n k_B T}{3\pi^2} \int_0^\infty dq \frac{f(q)}{\eta(q)}, \tag{2}$$

which reduces to Eq. (1) when simple models for the q-dependent shear viscosity $\eta(q) = (n k_B T/q^2) \times (\int_0^\infty C_T(q,t)dt)^{-1}$ are used [12]. Equation (2) is obtained using the identity $\int_0^\infty C_L(q,t)dt = 0$. This model therefore suggests that, although C_L contributes significantly to the time dependence of $Z(t)$ in the OCP, the OCP diffusion

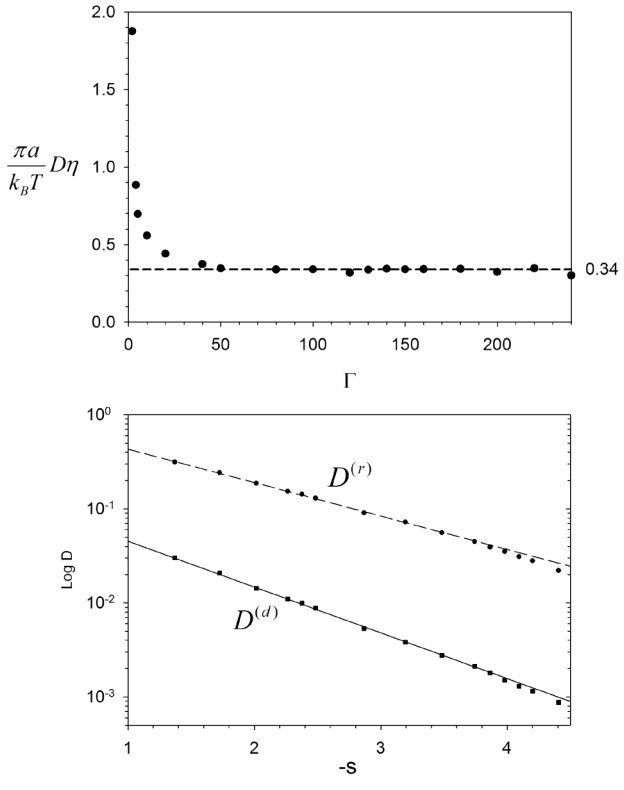

FIG. 3. (Top panel) Variation with Γ of the product $D\eta\pi a/k_B T$. (Bottom panel) Logarithm of $D^{(r)}$ and $D^{(d)}$ vs minus the excess entropy s. The lines are least squares fits.

coefficient should be controlled at high Γ by C_T, and therefore should satisfy a Stokes-Einstein relation. Figure 3 shows that, indeed,

$$D\eta\pi a/k_BT \simeq 0.341 \pm 1\%, \qquad \Gamma \geq 50. \tag{3}$$

In liquids experimental evidence tends to support the slipping boundary conditions $q = 4$ [10]. For the OCP, combining Eqs. (1) and (3) with $q = 4$ results in an effective radius $R \simeq 1.46a$, which compares well with the cage radius d^*; it nearly corresponds to the radius when $g(r)$ becomes larger than 1. As discussed in [7], Eq. (3) could be used to estimate the diffusion of impurities in compact astrophysical objects.

In an effort to provide a unifying quantitative description of atomic transport in condensed matter, it was shown that transport coefficients of liquids with quite disparate pair interactions satisfy universal relationships with equilibrium thermodynamic properties. Rosenfeld [13] first established a quasiuniversal behavior of the reduced diffusion $D^{(r)} = Dn^{1/3}/(k_BT/m)^{1/2}$ and viscosity $\eta^{(r)} = \eta/(n^{2/3}(mk_BT)^{1/2})$ as a function of the reduced excess entropy $s = S_{\rm ex}/Nk_B$ of the form $D^{(r)} \simeq 0.6e^{-0.8s}$ and $\eta^{(r)} \simeq 0.2e^{0.8s}$, for all dense ordinary fluids, $s \leq -1$ (freezing corresponds to about $-5 \leq s \leq -4$). Different potentials can be fitted better by somewhat different exponential arguments and prefactors; nevertheless, with the aforementioned relation, the diffusion coefficients of strongly coupled fluids are estimated within about 30%. For the OCP, we estimated s using the accurate equation of state of DeWitt and Slattery [14]. Figure 3 shows the plot of $D^{(r)}$ vs $-s$ for the OCP. The least squares fits over the $-4.4 \leq s \leq -1$ range (i.e., $50 \leq \Gamma \leq 200$) yields $D^{(r)} \simeq \alpha\exp(-\beta s)$ with $\alpha = 0.98 \pm 0.02$ and $\beta = 0.82 \pm 0.01$, in accordance with the above cited results. The identity $D^{(r)}\eta^{(r)} = (4/3\pi^2)^{1/3}D\eta\pi a/k_BT$ together with Eq. (3) yields $\eta^{(r)} \simeq 0.18\exp(\beta s)$ for $s \leq -2.26$, i.e., $\Gamma \geq 50$, also in agreement with Rosenberg's result. Recently, by recognizing that momentum and energy transfers at high densities are facilitated by the strong repulsion prevailing at small separations and that the rate of cage diffusion is proportional to the number of accessible configurations, Dzugutov [15] inferred that the reduced diffusion $D^{(d)} = D/(\Gamma_E\sigma^2)$ should be proportional to e^s. Here σ is the position of the first peak in $g(r)$ and $\Gamma_E = 4\sigma^2 g(\sigma)\rho\sqrt{\pi k_BT/m}$ is the Enskog collision frequency. In [15] Dzugutov approximated s by the two-body approximation $s_2 = -2\pi n\int_0^\infty [g(r)\log(g(r)) - (g(r) - 1)]r^2dr$, and obtained the scaling law $D^{(d)} = 0.049e^{s_2}$ for several model liquids. Then Hoyt *et al.* [16] showed that it is essential to use the actual s rather than the simple two-body approximation s_2, and obtained $D^{(d)} \propto e^{\alpha s}$ with $\alpha = 1.06 \pm 0.07$. Figure 3 shows $\mathrm{Log}D^{(d)}$ vs $-s$ for the OCP; the least squares fit yields a slope of -1.121 with an uncertainty of ± 0.018, in agreement with Hoyt's result. These results extend to long-range interactions, the unifying description of transport in condensed matter.

In summary, the OCP transport properties behave like *dense* ordinary liquids for $\Gamma > 50$ when caging is important. At smaller coupling, $\Gamma < 50$, even when the OCP exhibits the short-range order typical of liquids [oscillations in $g(r)$ arise when $\Gamma > 3$], the transport properties are driven by a complicated combination of kinetic and potential effects, which remain to be clarified. These results will be used to develop models of transport in more complex strongly coupled Coulomb systems, as is done with multicomponent liquids [16,17].

The author acknowledges useful discussions with M. S. Murillo in the early stage of the work. This research is supported by the Department of Energy, under Contract No. W-7405-ENG-36.

*Electronic address: daligault@lanl.gov

[1] M. Baus and J.-P. Hansen, Phys. Rep. **59**, 1 (1980).
[2] D. Levesque and L. Verlet, Phys. Rev. A **2**, 2514 (1970).
[3] U. Balucani, A. Torcini, and R. Vallauri, Phys. Rev. A **46**, 2159 (1992).
[4] Z. Donko, G. J. Kalman, and K. I. Golden, Phys. Rev. Lett. **88**, 225001 (2002).
[5] T. Gaskell and O. Chiakwelu, J. Phys. C **10**, 2021 (1977).
[6] P. Schmidt *et al.*, Phys. Rev. E **56**, 7310 (1997).
[7] C. J. Deloye and L. Bildsten, Astrophys. J. **580**, 1077 (2002).
[8] H. Eyring, J. Chem. Phys. **4**, 283 (1936).
[9] N. H. March and M. P. Tosi, *Introduction to Liquid State Physics* (Word Scientific, Singapore, 2002); see Table 6.2.
[10] R. Zwanzig, J. Chem. Phys. **79**, 4507 (1983).
[11] T. Gaskell, J. Non-Cryst. Solids **61**, 913 (1984); T. Gaskell and S. Miller, J. Phys. C **11**, 3749 (1978).
[12] If the q dependence of $\eta(q)$ is ignored, $\eta(q) = \eta$, Eq. (2) reduces to $D = \frac{k_BT}{4\pi\eta a}$; with the simple empirical law $\eta(q) = \eta(1 + \alpha^2q^2)^{-1}$ proposed for hard spheres [W. E. Alley and B. J. Adler, Phys. Rev. A **27**, 3158 (1983)], one obtains Eq. (1) with $R = a/[1 + 2(\alpha/a)^2]$.
[13] Y. Rosenfeld, J. Phys. Condens. Matter **11**, 5415 (1999); Phys. Rev. A **15**, 2545 (1977).
[14] H. DeWitt and W. Slattery, Contrib. Plasma Phys. **39**, 97 (1999).
[15] M. Dzugutov, Nature (London) **381**, 137 (1996).
[16] J. J. Hoyt, M. Asta, and B. Sadigh, Phys. Rev. Lett. **85**, 594 (2000).
[17] Y. Rosenfeld *et al.*, Phys. Rev. Lett. **75**, 2490 (1995).
[18] J. P. Hansen, I. R. McDonald, and E. L. Pollock, Phys. Rev. A **11**, 1025 (1975).